Trapping and cooling of ions

Caroline Champenois

These notes are part of the five lessons given in Les Houches on october 2008 for the cold atom and BEC predoc school. Why a lesson about trapped ions in such a school? There is no BEC, no degenerate gas, no Mott transition with trapped ions...but there are optical clocks among the most accurate in the world, there is phase transition from liquide to crystal, there are cold molecules to study cold reactions and most famous of all, there is the realisation of quantum gates, the bricks of quantum computer. Furthermore, experiments done with trapped ions have inspired and initiated several breakthroughs with neutral atoms because with such a system, "your hands are free", the trap keeps the ion(s) for you and you can try many different laser interaction protocoles. Here are the basics that, I hope, will help you understand why experiments with trapped ions can be so interested.

1 Confining charged particules with oscillating electric fields

1.1 The adiabatic approximation

Because of the Laplace law ruling a space free of charge ($\Delta V = 0$), it is not possible to trap a charged particule only by static electric field. For example, if by a set of electrodes a confining harmonic potential is created in the (x, y) plane, it has to be non-confining in the z direction:

$$\Phi(x, y, z) = A(x^2 + y^2 - 2z^2) \tag{1}$$

The idea of W. Paul was to use an oscillating potential

$$\Phi_{rf}(x, y, z, t) = A(x^2 + y^2 - 2z^2)\cos(\Omega t) \tag{2}$$

more generally, the potential is the sum of a radiofrequency and a static contribution:

$$\Phi(\mathbf{r}, t) = \Phi_{rf}(\mathbf{r}, t) + \Phi_s(\mathbf{r}, t) \tag{3}$$

The first radiofrequency ion trap worked in 1954 and the first paper where its principle was described was written by W. Paul in 1956 and mentionned an "ionenkäfig". Wolfgang Paul and Hans Dehmelt won the Nobel prize in physics in 1989 "For the development of the ion trap technique".

To understand the motion of an ion inside such a potential, let's first assume there is no static voltage ($\Phi_s(\mathbf{r}) = 0$). If the time oscillating electric field $\mathbf{E_0}(\mathbf{r})\cos(\Omega t)$ is uniform ($\mathbf{E_0}(\mathbf{r}) = \mathbf{E_0}$), then the motion is simply a rf driven motion at frequency Ω:

$$\mathbf{r}(t) = -\frac{q\mathbf{E_0}}{m\Omega^2}\cos(\Omega t) = -\mathbf{a}\cos(\Omega t) \tag{4}$$

But if $\mathbf{E_0}(\mathbf{r})$ is non uniform, the motion can be interpreted as the sum of a slow motion induced by the enveloppe of the rf field and the rf driven motion which has an amplitude

depending on the local rf field.

$$\mathbf{r}(t) = \underbrace{\mathbf{R_0}(t)}_{slow} + \underbrace{\mathbf{R_1}(t)}_{-\mathbf{a}(t)\cos(\Omega t)} \tag{5}$$

the local electric field ruling the equations of motion can be written like:

$$\mathbf{E_0}(\mathbf{r}(t)) = \mathbf{E_0}(\mathbf{R_0}) - (\mathbf{a}.\nabla)\mathbf{E_0}(\mathbf{R_0})\cos(\Omega t) + \cdots \tag{6}$$

A simple resolution can be reached by two approximations:

- a first order development of $\mathbf{E_0}$ around $\mathbf{R_0}$.
- **the adiabatic approximation** assuming that : *the typical evolution time scale of* $\mathbf{a}$ *and* $\dot{\mathbf{R}}_\mathbf{0}$ *is far longer than the rf period.*

with $\mathbf{a}(t) = \mathbf{a}(\mathbf{R_0}(\mathbf{t}))$ put into the equation, one can easily show that

$$m\ddot{\mathbf{R}}_\mathbf{0} = -\frac{Q^2}{4m\Omega^2}\mathbf{grad}(E_0^2). \tag{7}$$

It says that as far as $\mathbf{R}_0(t)$ is concerned, it is like the particle is trapped in a static potential well called the **pseudopotential**:

$$V^*(\mathbf{r}) = \frac{Q^2E_0^2(\mathbf{r})}{4m\Omega^2}. \tag{8}$$

If the static electric field is switched on again, the superposition principle leads to the effective potential

$$V^*_{eff}(\mathbf{r}) = \frac{Q^2E_0^2(\mathbf{r})}{4m\Omega^2} + q\Phi_s(\mathbf{r}) \tag{9}$$

and the motion in this potential gives $\mathbf{R}_0(t)$. The rf-driven motion (μmotion) is deduced by

$$\mathbf{R_1}(t) = -\frac{Q\mathbf{E_0}(\mathbf{R_0})}{m\Omega^2}\cos(\Omega t) \tag{10}$$

The potential $V^*(\mathbf{r})$ effectively traps if $E_0^2(\mathbf{r})$ increases with r (this condition is not sufficient, see further). So the further is the ion from the center of the trap, the larger is the μmotion. The μmotion being a driven motion proportionnal to the local field, it can not be cooled.

1.2 Choosing a geometry, the quadrupole as a generator of harmonic potential

Let's go back to our first goal: create a harmonic trapping potential in 3D for a charged particle. Now, we know we have to make a detour to rf field and make sure that $E_0^2(\mathbf{r})$ and $\Phi_s(\mathbf{r})$ behave like (x^2, y^2, z^2). This is reached if

$$\Phi_{rf}(\mathbf{r}, t) = -(\alpha x^2 + \beta y^2 + \gamma z^2)\cos(\Omega t). \tag{11}$$

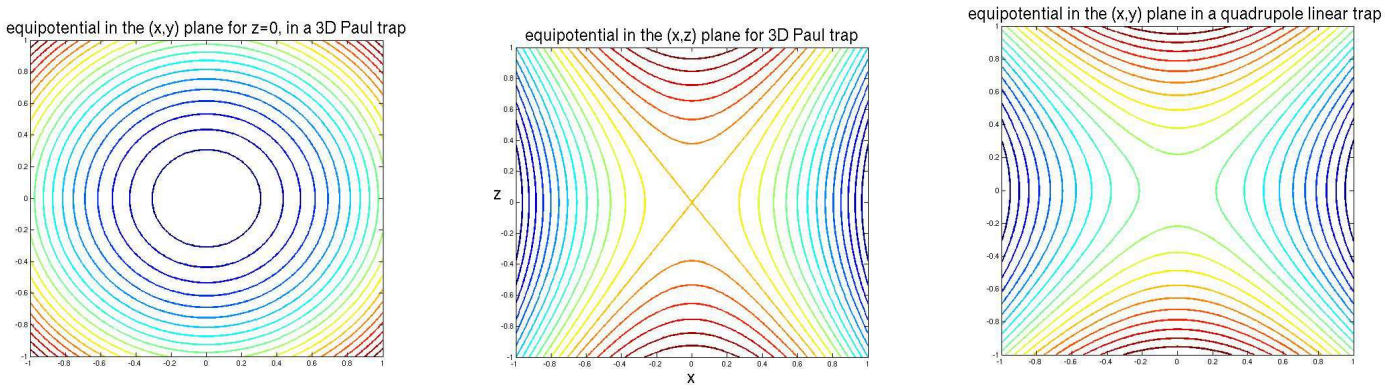

Figure 1: On the left, equipotential in the $x-y$ plane of a indeal 3D Paul trap (axis of symmetry: Oz). in the center, equipotential in the $x-z$ plane for the same trap, on the right, equipotential in the $x-y$ plane of an ideal linear rf-trap.

with $\alpha+\beta+\gamma=0$. Two geometries with two different symmetries are used; the 3D cylindrical trap where $\alpha=\beta=-\gamma/2$ and the 2D translational symmetry where $\alpha=-\beta, \gamma=0$ and where a static voltage is required to trap along the Oz axis (see figure 1 for equipotential lines in both geometries). Let's first deal with the 3D geometry, many points can be extrapolated to the 2D linear geometry. In 3D, the ideal geometry is a ring plus two endcaps. If a static voltage is added to the rf voltage and both are applied between the ring and the two endcaps, the potential voltage created between the electrodes can be described by

$$\Phi(\mathbf{r},t)=(V_0\cos(\Omega t)+V_s)\frac{x^2+y^2-2z^2}{2r_0^2}. \tag{12}$$

where r_0 is the radius of the trap (see figure 2). Such a voltage repartition can be produced if the surfaces of the electrodes exactly match an equipotential surface which is an hyperboloid of revolution (x^2-2z^2 =constante)(see fig 2).

But even if the trap is perfectly machined, it is never like in the equations, simply because the trap has a finite size. Today, several experiments even use miniature (see fig 2, right) and micro traps which do not obey the perfect geometry required by equations. Nevertheless, as long as some symmetry principles are obeyed, in the center of the trap, the potential created by the electrodes can be approximated by equation (12). Getting further from the trap center, higher order contributions become non negligeable. This is of importance for experiments with a large set of ions, where areas far from the center are visited by the ions.

In the following, we assume Eq (12) is a good representation of the voltage. In the adiabatic approximation, the effective potential is then

$$V^*_{eff}(\mathbf{r})=\frac{Q^2V_0^2}{4m\Omega^2r_0^4}(x^2+y^2+4z^2)+\frac{QV_s}{2r_0^2}(x^2+y^2-2z^2) \tag{13}$$

(here we use the convention where V_0 and V_s are potential differences between the ring and the end-caps forming the trap). Inside this harmonic potential, the motion can be

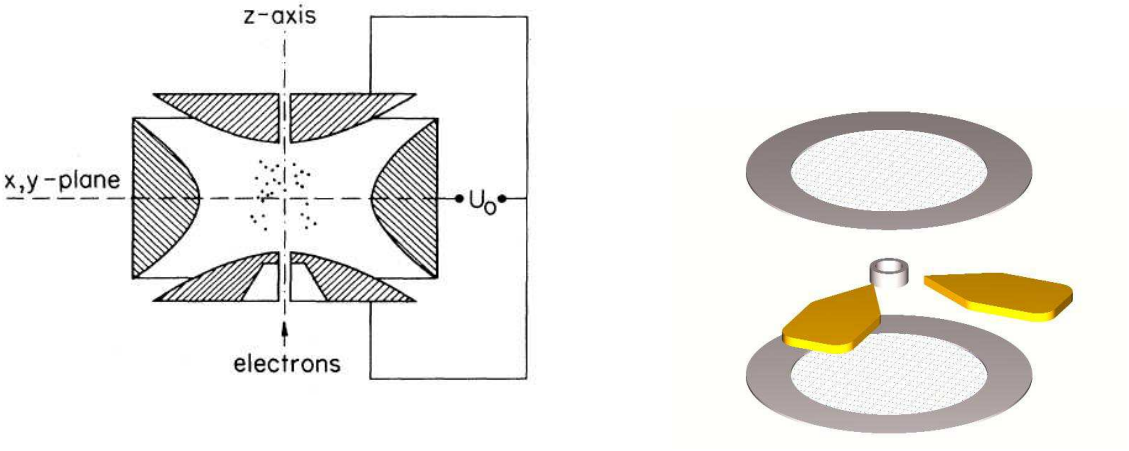

Figure 2: On the left, a Paul trap like shown by Paul in his Nobel lecture, $2r_0$ is the smallest inner diameter of the ring. For an ideal geometry, the height $2z_0$ between the two endcaps should be equal to $2\sqrt{2}r_0$. On the right, an example of a miniature trap, the ring inner diameter is 1.4 mm.

described by two frequencies of motion (one for x, y and one for z). Some parameters are very useful to define these frequencies and other things:

$$q_x = -\frac{2QV_0}{m\Omega^2 r_0^2} \quad ; \quad q_z = \frac{4QV_s}{m\Omega^2 r_0^2} \tag{14}$$

$$a_x = \frac{4QV_s}{m\Omega^2 r_0^2} \quad ; \quad a_z = -\frac{8QV_s}{m\Omega^2 r_0^2} \tag{15}$$

From these parameters, the frequencies of motion can be expressed like:

$$\omega_x = \frac{\Omega}{2}\sqrt{a_x + q_x^2/2} \quad ; \quad \omega_z = \frac{\Omega}{2}\sqrt{a_z + q_z^2/2} \tag{16}$$

Following our construction of macro and micromotion, the equation of motion of a single ion in such a trap is then

$$x(t) = X\cos(\omega_x t)\left(1 + \frac{q_x}{2}\cos(\Omega t)\right) \tag{17}$$

1.3 Beyond the adiabatic approximation

In the particular case of a quadrupolar geometry (where the pseudopotential is harmonic), the complete equations of motion **for a single ion** can be solved analytically, without any approximation. In a potential described by Eq 12, the equations of motion are **linear** and **uncoupled** in the spatial coordinates (it is not true for higher order geometries). So each coordinates can be studied independantly:

$$\ddot{x} = -\frac{Qx}{mr_0^2}(V_0\cos\Omega t + V_s) \tag{18}$$

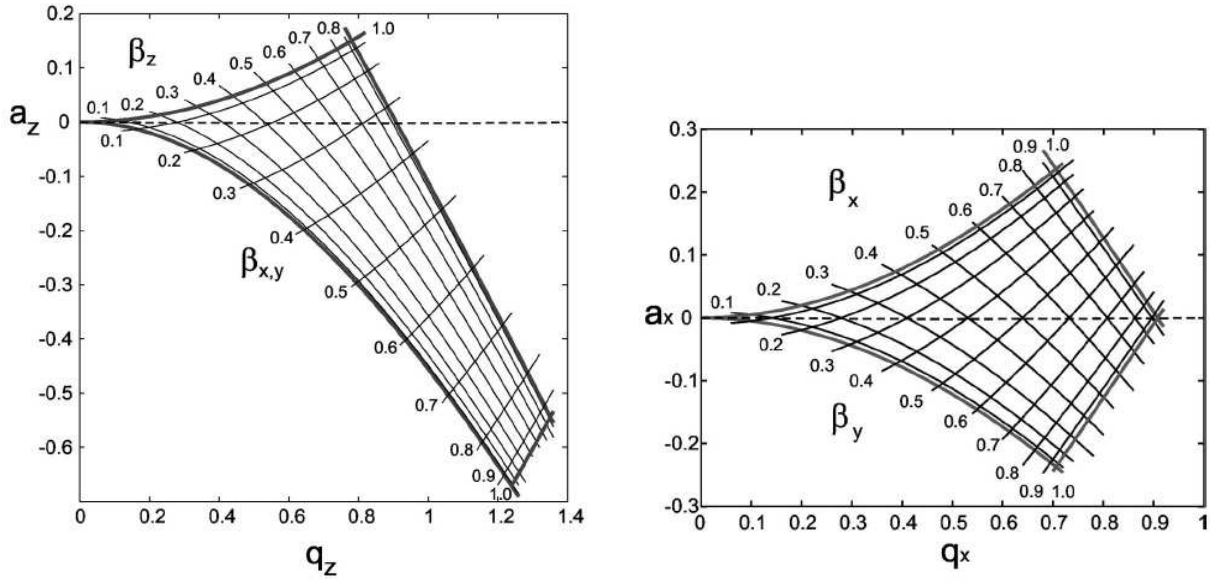

Figure 3: Stability region of the Mathieu equation where rf traps are operated, left: 3D Paul trap, right: linear trap.

the introduction of the reduced time scale $\xi = \Omega t/2$ leads to the well-known Mathieu equation

$$\frac{\mathrm{d}^2x}{\mathrm{d}\xi^2} + (a_x - 2q_x\cos(\Omega t))x(\xi) = 0 \tag{19}$$

which belongs to the family of differential equations with periodic coefficients. Solutions of this equation can be found in many math textbooks. The important points to remember are

- the solutions have the form

$$x(t) = Ae^{i\omega_x t}\sum_n C_{2n}e^{in\Omega t} + Be^{-i\omega_x t}\sum_n C_{2n}e^{-in\Omega t} \tag{20}$$

  with $\omega_x = \beta_x\Omega/2$, β_x depending only on a_x and q_x.

- these solutions are stable if the $0 \leq \beta_i \leq 1$. This condition defines areas in the plane defined by (a_x,q_x) or (a_z,q_z): the stability regions. In practise, rf traps are operated in the lowest stability region (the one including (0,0), see figure 3).

The solutions of the Mathieu equation can be expanded in the lowest order approximation which requires $(|a_x|, q_x^2) \ll 1$ and then $\beta_x \ll 1$. In this limit

$$\beta_x = \sqrt{a_x + \frac{q_x^2}{2}} \tag{21}$$

and

$$x(t) = X\cos(\omega_x t)\left(1 + \frac{q_x}{2}\cos\Omega t\right) \tag{22}$$

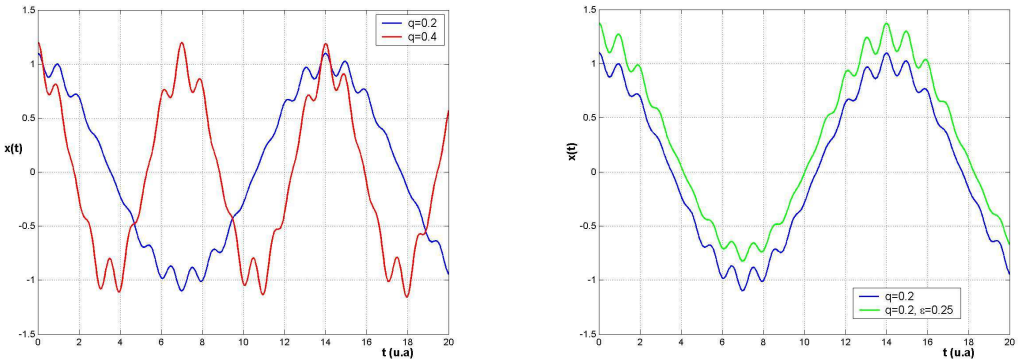

Figure 4: Left: plot of equation $X\cos(\omega_x t)\left(1+\frac{q_x}{2}\cos\Omega t\right)$ for $q_x = 0.2$ and 0.4. Right: plot of the same equation with $X\cos\omega_x t \rightarrow X(\epsilon_x + \cos\omega_x t)$ which includes an excess micromotion characterized by $\epsilon_x = 0.25$.

this is exactly the equation obtained in the adiabatic approximation. To have a look at examples of trajectories, go to figure 4. For an ideal 3D Paul trap, $a_z = -2a_{x,y}$ and $q_z = -2q_{x,y}$. This implies, for example, that if $V_s = 0$, $\omega_z = 2\omega_x$.

As soon as there is more than one ion in the trap, the Mathieu equation does not describe exactly the motion of the ions because it does not include the Coulomb repulsion. This repulsion becomes important when ions are cooled and when the ion-ion distance is reduced. Then, the equations of motion become nonlinear. The nonlinearities can manifest themselves by nonlinear resonance coupling the motion along x,y and z or coupling these motions to the radiofrequency. For some working parameters, the trajectories are then unstable, even inside the stability diagram. Imperfections in the shape of the electrodes can have the same effects.

1.4 Another tool to trap charged particles: the Penning trap

This device, invented by Penning already in 1936 makes use of a large magnetic field superposed to a static voltage applied on electrodes. The geometry can be a cylinder with two endcaps but many experiments now use the hyperboloid of revolution already defined for the Paul trap. The motion is characterized by three frequencies of motion. The oscillation in the static confining potential along Oz and two frequencies of motion for the plane $x-y$, related to the cyclotron and magnetron motion.

This device is very famous for the high precision measurement of $g-2$ for the electron (the first ones from 1969 to 1977 by Gräff and Dehmelt and the last one in 2006 by the group of Gabrielse (Harvard)). The other application of Penning trap is high precision mass measurement where the precision is such that the mass difference between isobare can now be exploited.

Because of the required high magnetic field, Penning traps are not very appropriate for most high precision spectroscopic measurements as a small relative fluctuation of the

magnetic field induces too high frequency fluctuations in the transition). To know more about them, refer to the books speaking about charged particle traps.

2 Interaction of light with ions trapped in a rf quadupole trap

When a high number of ions is trapped and the motion can no more be described by a harmonic oscillator+μmotion, the ion-light interaction is very similar to the ones of unbound atoms and concepts and processes known for neutral atom work roughly in the same way (Doppler cooling...). The situation becomes peculiar for single ion or single ions (a chain in a linear trap) which are trapped at the node of the rf field. Furthermore, if traps are operated with a_x and $q_x^2 \ll 1$ the motion can be very well described by a harmonic oscillator. Then, it becomes possible to coherently couple the internal and external degrees of freedom. Indeed, the Hamiltonian of the system can, in this limit, be equivalent to the Jaynes-Cummings Hamiltonian describing photons in QED cavity and several experiments with trapped ions have been inspired by this analogy (creation of non-classical states of vibration, coherent states...). In this section, we consider single ion(s) in quadrupole traps where the oscillation is characterized by $\omega_x, \omega_y, \omega_z$ and most of the time, we treat the atom as a two level system.

2.1 Classical treatment of the motion

The atom is considered as a two level system $|g\rangle, |e\rangle$ with internal energy $E_e - E_g = \hbar\omega_0$. The Hamiltonian of the non-interacting atom is

$$\hat{H}_0 = \frac{\hbar\omega_0}{2}\left(|e\rangle\langle e| - |g\rangle\langle g|\right) + \frac{p^2}{2m} \tag{23}$$

As a first step, the motion is treated classically and the laser-atom interaction Hamiltonian can be written like

$$\hat{V} = \frac{\hbar\Omega_L}{2}\left(|e\rangle\langle g| + |g\rangle\langle e|\right)\left(e^{i(\omega_L t - k_L x - \psi)} + c.c.\right) \tag{24}$$

The self evolution of the system can be eliminated by moving to the Interaction picture where $\hat{V}^I = \hat{\mathcal{U}}_0^\dagger(t)\hat{V}\hat{\mathcal{U}}_0(t)$. When doing this transformation, you see that the terms $|e\rangle\langle g|$ introduces $\exp(-i\omega_0 t)$ while $|g\rangle\langle e|$ introduces $\exp(i\omega_0 t)$. So the coupling hamiltonian $\hat{V}^I$ includes terms like $\exp(\pm i(\omega_0 + \omega_L)t)$ which rotate very fast and quasi resonant terms like $\exp(\pm i(\omega_0 - \omega_L)t)$. Like very often in atom-laser interactions, we keep into account only these quasi-resonant terms and do the Rotating Wave Approximation (RWA). In this approximation,

$$\hat{V}^I = \frac{\hbar\Omega_L}{2}\left(|e\rangle\langle g|e^{-i\delta t}e^{i(k_L x + \psi)} + |g\rangle\langle e|e^{i\delta t}e^{-i(k_L x + \psi)}\right) \tag{25}$$

this is a general expression for atom-laser interaction where the position of the atom inside the travelling wave is relevant. What's more for an oscillating ion?

In our case, the motion is well described by

$$x(t) = X\cos(\omega t)\left(1 + \frac{q}{2}\cos\Omega t\right) \tag{26}$$

for each axis of the trap. Let's first assume than

1. the laser propagates along one of this symmetry axis : $\mathbf{k}_L \parallel Ox$.
2. $q \ll 1 \rightsquigarrow x(t) \simeq X\cos(\omega t)$

Then the phase modulation implied by the motion of the ion to the atom-laser coupling is periodic, resulting in something like diffraction by a grating but in the time domain:

$$e^{ik_L x} = e^{ik_L X\cos\omega t} = \mathcal{J}_0(k_L X) + i\mathcal{J}_1(k_L X)e^{\pm i\omega t} - \mathcal{J}_2(k_L X)e^{\pm i2\omega t}... \tag{27}$$

where the $\mathcal{J}_n$ are the Bessel functions. So it is like the atom is excited by several lasers with frequency ω_L, $\omega_L \pm \omega$, $\omega_L \pm 2\omega$...with the coupling strength $\Omega_L.\mathcal{J}_0(k_L X)$, $\Omega_L.\mathcal{J}_1(k_L X)$, $\Omega_L.\mathcal{J}_2(k_L X)$. The index of modulation $k_L X$ controls the relative strength of each excitation and the number of bands that it is relevant to take into account (roughly, one can remember that $\mathcal{J}_n(u)$ becomes non negligeable when u is at least equal to n). In the non saturated case where the light-shift induced by a band (most probably the carrier) on its neighbour bands can be neglected, the excitation by this multiple frequency excitation can be solved for each band independently, which, for a two level atom, gives:

$$P_e(\delta) = \sum_{n=-\infty}^{n=+\infty} \frac{1}{2}\frac{\Omega_L^2\mathcal{J}_n^2(k_L X)}{\Omega_L^2\mathcal{J}_n^2(k_L X) + 2(\delta - n\omega)^2 + \Gamma^2/2} \tag{28}$$

When looking at such a spectrum for several configurations (like shown on figure 5), one can notice that

- for excitation on a broad transition ($\Gamma > \omega$), the oscillating nature of the motion is not very relevant to describe the spectrum.
- indeed, it can be shown that for $\Gamma \gg \omega$, the ions can be treated as free (regime often called the "weak binding regime").
- for $\Gamma < \omega$ (the "strong binding regime"), the sideband spectrum is a very efficient experimental tool to quantify the motion of the ion, *as long as there are not too many bands* and it is possible to point the central band without error. That's why every sideband spectrum always follows a Doppler cooling process.
- for $\Gamma < \omega$ and for a low amplitude of oscillation and then a low temperature, this classical description of the motion is not sufficient to explain the observed spectrum.

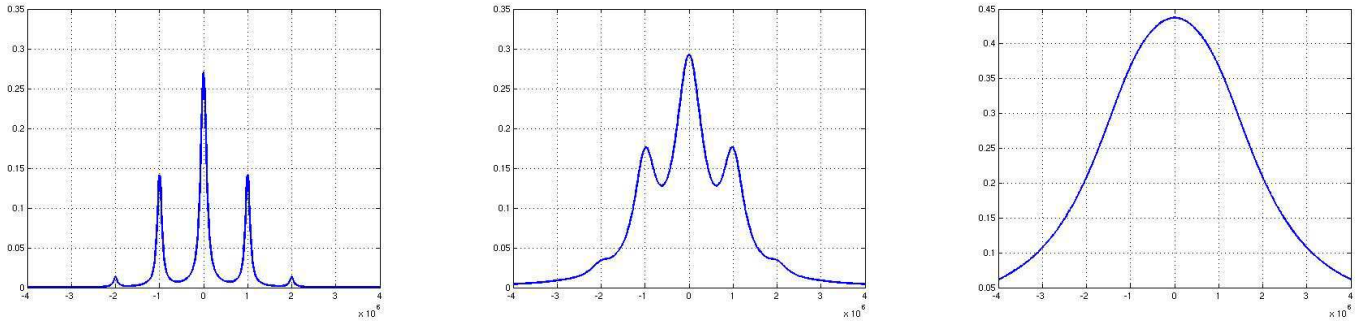

Figure 5: Calculated spectrum of a two level oscillating atom, the laser-atom interaction is characterized by $k_L X = 1$, $\omega/2\pi = 1$ MHz, $\Omega_L = \Gamma$. left: $\Gamma/2\pi = 10^5$ Hz, middle: $\Gamma/2\pi = 5.10^5$ Hz, right: $\Gamma/2\pi = 2.10^6$ Hz.

In a realistic experiment, the laser does not propagate along a symmetry axis of the trap and the motion can include non negligeable μmotion and even excess μmotion. Then

$$\mathbf{k}_L.\mathbf{r} = k_x(X\cos\omega_x t + \epsilon_x)(1 + \frac{q_x}{2}\cos\Omega t) + k_z(Z\cos\omega_z t + \epsilon_z)(1 + \frac{q_z}{2}\cos\Omega t) \qquad (29)$$

and the same spectral decomposition in Bessel function can be done with several frequencies, as long as these frequencies are not in a rational ratio.

2.2 Being in the strong binding regime

There are two ways to reach this regime :

- choose an ion with a dipole forbidden transition. In several cases, it is an electric quadrupolar transition ($S \rightarrow D$), with natural linewidth ≤ 1 Hz. This is the case for Ca^+, Sr^+, Ba^+, Ra^+, Yb^+, Hg^+. Let's also mentionned experiment with In^+, making use of an intercombination line.

- use Raman coupling between two sublevels (Zeeman or hyperfine) of the ground state. This is the case for Be^+, Mg^+, Zn^+, Cd^+.

2.3 The quantum description of the motion and the Lamb-Dicke regim

If the motion can be well described by a harmonic oscillator (one for each axis of the trap), it can be relevant to use a quantum description of the motion, especially when the motion is cooled down so few vibrational levels are populated. Then, the kinetic + potential energy have to be included in the Hamiltonian :

Summary of useful equations for H.O:

$$\hat{H}_0^m = \frac{\hat{p}^2}{2m} + \frac{m\omega^2}{2}\hat{x}^2 \Rightarrow \hat{H}_0^m = \hbar\omega(\hat{a}^\dagger\hat{a} + \frac{1}{2}) \qquad (30)$$

$$\begin{aligned}\hat{x} &= \sqrt{\frac{\hbar}{2m\omega}}(\hat{a}^\dagger + \hat{a}) = x_0(\hat{a}^\dagger + \hat{a}) \\ \hat{p} &= i\sqrt{\frac{m\hbar\omega}{2}}(\hat{a}^\dagger - \hat{a}) \end{aligned} \tag{31}$$

$$[\hat{a}, \hat{a}^\dagger] = \hat{1} \quad \hat{N} = \hat{a}^\dagger\hat{a} \tag{32}$$

$$\begin{aligned}\hat{a}^\dagger|n\rangle &= \sqrt{n+1}|n+1\rangle \\ \hat{a}|n\rangle &= \sqrt{n}|n-1\rangle \end{aligned} \tag{33}$$

To move again to the interaction picture, the self Hamiltonian of the system is now $\hat{H}_0 + \hat{H}_0^m$:

$$\hat{V}^I = \frac{\hbar\Omega_L}{2}\left(|e\rangle\langle g|e^{-i(\delta t-\psi)}e^{i\hat{H}_0^m t/\hbar}e^{ik_L\hat{x}}e^{-i\hat{H}_0^m t/\hbar} + H.c.\right) \tag{34}$$

with $\hat{x} = x_0(\hat{a} + \hat{a}^\dagger)$. By using the relation

$$e^{\hat{A}+\hat{B}} = e^{\hat{A}}e^{\hat{B}}e^{-1/2[\hat{A},\hat{B}]} \quad \text{if} \quad [\hat{A},[\hat{A},\hat{B}]] = [\hat{B},[\hat{A},\hat{B}]] = 0 \tag{35}$$

and by using $\exp(\hat{A}) = \hat{1} + \hat{A} + \hat{A}^2/2 + \hat{A}^3/6 + \ldots$ one can demonstrate these useful relations to move to the interaction picture:

$$\hat{a}^n e^{-i\omega\hat{a}^\dagger\hat{a}} = e^{-i\omega\hat{a}^\dagger\hat{a}}e^{-in\omega t}\hat{a}^n \tag{36}$$

$$\hat{a}^{\dagger n} e^{-i\omega\hat{a}^\dagger\hat{a}} = e^{-i\omega\hat{a}^\dagger\hat{a}}e^{in\omega t}\hat{a}^{\dagger n} \tag{37}$$

$$e^{i\eta(\hat{a}+\hat{a}^\dagger)} = e^{i\eta\hat{a}}e^{i\eta\hat{a}^\dagger}e^{-\eta/2} \tag{38}$$

and then, finally:

$$\hat{V}^I = \frac{\hbar\Omega_L}{2}\left(|e\rangle\langle g|e^{-i(\delta t-\psi)}\exp\left(i\eta\hat{a}^\dagger e^{i\omega t} + i\eta\hat{a}e^{-i\omega t}\right) + H.c.\right) \tag{39}$$

with $\eta = k_L x_0$, the Lamb-Dicke parameter (x_0 is the size of the ground vibrational wavepacket). The Hamiltonian $\hat{V}^I$ allows to couple internal and external degrees of freedom by one laser pulse. The eigenstates of the non coupled Hamiltonian $\hat{H}_0 + \hat{H}_0^m$ are now $|g\rangle|n\rangle, |e\rangle|m\rangle$. Here, we care only about one H.O. eigenstates but it can be easily generalized to full 3D H.O. by introducing n_x, n_y, n_z. For each transition modifying the vibrational state, an effective Rabi frequency can be defined by

$$\Omega_{n,n+p} = \Omega_L|\langle n+p|e^{i\eta(\hat{a}+\hat{a}^\dagger)}|n\rangle| \tag{40}$$

This expression can be found developped in a paper by Glauber in 1969: for $p \geq 0$

$$\Omega_{n,n+p} = \Omega_L e^{-\eta^2/2}\eta^p\sqrt{\frac{n!}{(n+p)!}}\mathcal{L}_n^p(\eta^2) \tag{41}$$

We can gain more insight by making a Taylor expansion of $\hat{V}^I$ with η. Up to the second order in η:

$$
\begin{array}{ll}
n \to n & \Omega n, n = \Omega_L(1-\eta^2 n) \\
n \to n+1 & \Omega n, n+1 = \Omega_L \eta\sqrt{n+1} \\
n \to n-1 & \Omega n, n-1 = \Omega_L \eta\sqrt{n} \\
n \to n+2 & \Omega n, n+2 = \Omega_L \eta^2/2\sqrt{(n+1)(n+2)} \\
n \to n-2 & \Omega n, n-2 = \Omega_L \eta^2/2\sqrt{n(n-1)}
\end{array}
$$

This development shows that the $p-$sideband couplings scale like $(\eta\sqrt{n})^p$. For $\eta\sqrt{n} \ll 1$, the second order excitations are negligeable and only the first sidebands are excited. This is the **Lamb-Dicke** regime which corresponds formaly to the validity regime of $\exp ikx = 1 + ikx$. Many experiments implying high precision spectroscopy (QI, metrology...) requires to reach this regime where the Doppler spectra is reduced to the main carrier (central) band and small first order sideband, with a broadening/shift only induced by the second order Doppler effect.

The amplitude of one band in the spectrum is the sum of many contributions, starting from all the populated vibrational levels. The occupation probability $P(n)$ depends on the process applied to prepare the motional state of the ion. For example, Doppler cooling results in a thermal distribution of n. To have an order of magnitude, with usual miniature trap for single ions, the Doppler cooling allows to reach a thermal distribution caracterised by $\overline{n} \simeq 5-15$. Then it takes $\eta \ll 1$ to reach $\eta\sqrt{\overline{n}} < 1$ after a Doppler cooling process. This has to be already thought of when the trap is designed. As

$$\eta = \frac{2\pi}{\lambda}\sqrt{\frac{\hbar}{2m\omega}} \tag{42}$$

λ ranges from 282 nm (Hg^+) $\to$ 729 nm (Ca^+) $\to$ 1760 nm (Ba^+). m ranges from $m = 9$ (Be^+) to $m = 199$ (Hg^+) and $m = 226$ (Ra^+) . For Raman coupling k_{eff} can be made very small (and so the effective λ very big) and η can be modified by adjusting laser direction of propagation.

But **how to make high ω ?** This is a major issue for ion trappers as it offers two advantages:

- for a given atom (mass and transition) it makes η smaller.
- for a given temperature, for example, reached by Doppler cooling, the averaged occupation number $\overline{n}$ is smaller ($\overline{n} = \exp(-\hbar\omega/k_BT)/(1-\exp(-\hbar\omega/k_BT))$).

In the case where no static potential are applied, in the adiabatic approximation, the oscillation frequency is

$$\omega_x = q_x/2\sqrt{2}\Omega = 1/2\sqrt{2}\frac{2QV_0}{m\Omega^2 r_0^2}\Omega \tag{43}$$

For stability reason and to remain in the adiabatic approximation, q_x is bounded : $0 < q_x \leq 0.2 - 0.4$ (depending on experiment). So for a given q_x, reaching high ω_x implies using high Ω. The order of magnitude for Ω, for high precision spectro experiment (optical clock, QC processes) is $\Omega \simeq 10-40$ MHz. It is technically very difficult to keep q_x around

0.1-0.2 as q_x scales like $1/\Omega^2$ and so the amplitude voltage V_0 should be increased to compensate that. Technically V_0 is limited to few 1000 V so the other way is to reduce r_0, the size of the trap. Tis explains why, in the 90's, there was a move from centimeter trap to millimeter trap.

Now, let's assume the trap is designed so that doppler cooling is sufficient to reach the **Lamb-Dicke (LD) regime**. The LD regime is when the phase modulation $|k_L x(t)|$ is small enough so that its effect on the laser-atom interaction can be simplified by $\exp(ik_L x(t)) \simeq 1 + ik_L x(t)$. Then the interaction Hamiltonian is simply

$$\hat{V}^I = \frac{\hbar\Omega_L}{2}|e\rangle\langle g|\left(\hat{1}e^{-i(\delta t-\psi)} + i\eta\hat{a}^\dagger e^{-i(\delta-\omega)t-\psi} + i\eta\hat{a}e^{-i(\delta+\omega)t-\psi} + H.c.\right) \tag{44}$$

the laser interaction reduced to three componants:

$$\begin{aligned} n \to n \quad & \Omega n, n = \Omega_L \\ n \to n+1 \quad & \Omega n, n+1 = \Omega_L\eta\sqrt{n+1} \\ n \to n-1 \quad & \Omega n, n-1 = \Omega_L\eta\sqrt{n} \end{aligned}$$

and when $n \gg 1$, $\Omega_{n,n+1} \simeq \Omega_{n,n-1}$. As $\Omega_{n,n\pm1}$ depends on n, the excitation has to be calculated for each n and weighted by $P(n)$. If the ion has been laser cooled, it is very well represented by a thermal state

$$P(n) = \frac{1}{1+\overline{n}}\left(\frac{\overline{n}}{1+\overline{n}}\right)^n. \tag{45}$$

Be aware that this state is not formally equivalent to $X\cos(\omega t)$ which is rather equivalent to a coherent state (cf quantum optics coherent states or Glauber states). The thermal state is an uncoherent superposition of coherent states with distribution of amplitude X like

$$P(X)\mathrm{d}X = X/\sigma^2 \exp\left(-\frac{X^2}{2\sigma^2}\right)\mathrm{d}X \tag{46}$$

with $E_{th} = m\omega^2\sigma^2$ (see Eschner, EPJD **22** (2003)). The coherent state has been invented by Glauber for laser field $\mathcal{E}\cos\omega t$. It can be described by its representation in the $|n\rangle$ basis:

$$|\alpha\rangle = e^{-|\alpha^2|/2}\sum_0^\infty \frac{\alpha^n}{\sqrt{n!}}|n\rangle \tag{47}$$

and then $\overline{n} = |\alpha|^2$. The averaged position on such a coherent state is

$$\langle x\rangle_\alpha = x_0(\alpha+\alpha^*) = 2x_0|\alpha|\cos(\omega t+\phi) \tag{48}$$

So you can connect the physical values by $X = 2x_0\sqrt{\overline{n}}$ and $V = X\omega$ so

$$1/2mV^2 = \overline{n}\hbar\omega \tag{49}$$

Coming back to the thermal distribution, the on-resonance probability of excitation on the $\Delta n = +1$ band ($\delta = +\omega$), called the first blue side band (or 1BSB) is,

$$S_{BSB} = \sum_0^\infty P(n)\frac{1}{2}\frac{\Omega_L^2\eta^2(n+1)}{\Omega_L^2\eta^2(n+1)+\Gamma^2/2} \tag{50}$$

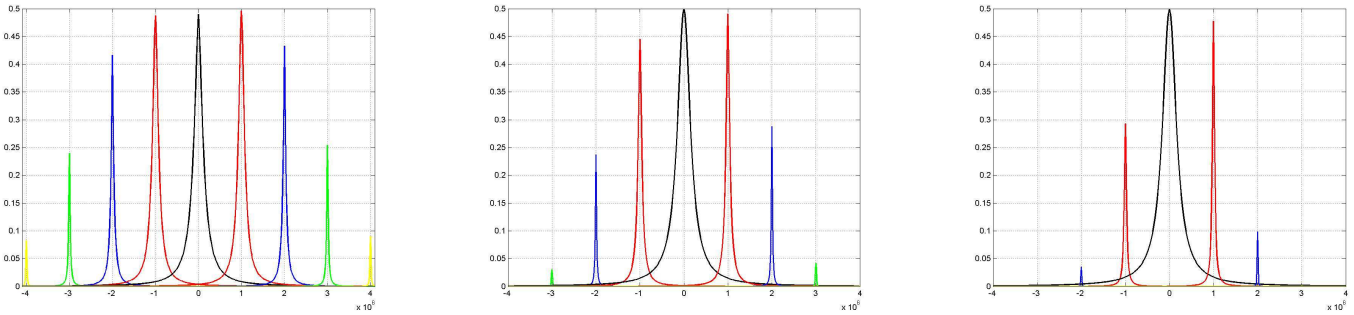

Figure 6: Calculated spectra of a $^{40}Ca^{+}$ ion with thermal distribution of n and the Laguerre polynomial developpement for the effective Rabi frequencies. $\Omega/2\pi = 1$ kHz, the laser linewidth $\Gamma_L/2\pi = 10$ kHz ,$\lambda_L = 730$ nm, $\omega/2\pi = 1$ MHz : $\eta_0 = 0.094$. left: $T = 2.5$ mK and $\overline{n} = 51.6$, center: $T = T_D = 0.5$ mK, $\overline{n} = 10$,right $T = 0.1$ mK $\overline{n} = 1.6$. With a lower Rabi frequency, the second order sidebands are already very small for $T = T_D$.

The on-resonance probability of excitation on the $\Delta n = -1$ band ($\delta = -\omega$), called the first red side band (or 1RSB) is,

$$S_{RSB} = \sum_{1}^{\infty} P(n) \frac{1}{2} \frac{\Omega_L^2 \eta^2 n}{\Omega_L^2 \eta^2 n + \Gamma^2/2} \tag{51}$$

$$= \sum_{0}^{\infty} P(n+1) \frac{1}{2} \frac{\Omega_L^2 \eta^2 (n+1)}{\Omega_L^2 \eta^2 (n+1) + \Gamma^2/2} \tag{52}$$

$$= \frac{\overline{n}}{1+\overline{n}} S_{BSB} \tag{53}$$

because $P(n+1) = \overline{n}/(1+\overline{n})P(n)$. This last relation is very important as it is independant of the atomic or laser parameters and it offers a very efficient way to measure experimentally $\overline{n}$ by comparing the two sidebands. This difference between blue and red sideband is visible on the calculated spectra shown on figure 6 and is the signature of the motion quantum regime. When $\overline{n} \to 0$ the amplitude of the RSB$\to 0$ as there is no red transition from $n = 0$. But how to realise such sideband spectra on transition which emits on average one photon per second?

2.4 Detection of the internal state

Making a resolved sideband Doppler spectrum means $\Gamma \ll \omega$. In practise, for transition like the $S \to D$, the spontaneous decay rate is of the order of 1 /s...we can not base the measurement method on detection of these photons! The method to deal with that issue was invented by H. Dehmelt (Nobel Prize 1989) and is called the **electron shelving method**. It makes use of a particular internal structure that can be shaped as a V. The ground state $|g\rangle$ is coupled by a dipole allowed transition to state $|e\rangle$ and to the metastable state $|m\rangle$ by a dipole forbidden transition. On the dipole allowed transition,

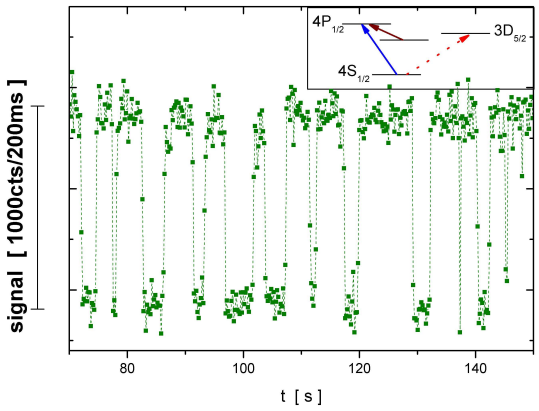

Figure 7: Quantum jump signal measured in the fluorescence emitted by a single calcium ion and the lasers required to observe this signal (two lasers for Doppler cooling,one principal and one repumper, one laser for shelving the electron).

the scattering rate is high (typically 10 000-50 000 c/s measured) whereas on the dipole forbidden transition the relevant evolution timescale is very long ($\geq$ 100 ms). So when the lasers coupling on these two transitions are shined to a single ion, the signal can only have two values (see figure 7). Or the atom is in $|g\rangle - |e\rangle$ subspace and the signal is high, or it is excited to the metastable state and it stays there for a long time (one second on average), it is "shelved" and can not be excited on the dipole allowed transition: the signal is low (only background light). These dark periods are the signature of the ion being in the $|m\rangle$ state. The fact that the signal has only two possible values is the signature that there is only one ion in the trap. The first experimental observations of electron shelving were done in 1986 in three labs, the NIST group (D. Wineland, W. Itano, J. Bergquist and coworkers), the group of Dehmelt in H. Washington and the group of P. Toschek in Hamburg.

To do a resolved sideband spectrum, the method described above is not exactly the good one because the AC Stark effect (or light- shift) due to the dipole allowed (DA) transition broadens too much the dipole forbidden (DF) transition. The two laser excitation have to be sequential. After excitation on the DF transition, the ion has probability p_m to be in the metastable state. When the laser on the DA transition in ON, there is a state measurement which project the internal state into either $|g\rangle$ or $|m\rangle$. This projection implies an uncertainty to the measurement, called the Quantum Projection Noise (QPN). After a coherent excitation, the variance associated to the state measurement is $p_m(1-p_m)$ and then the minimal noise is $\sqrt{p_m(1-p_m)}$. So several measurements have to be done at the same frequency to reach good statistics (typically 100 measurements). Taking into account that a measurement run takes rougthly 10 ms, it takes 10 s per points and more than an hour for the full sideband spectrum! So the laser on the DF transition has to be spectrally narrow and very stable not to drift during

this spectrum by more than a step (typically 1 kHz).

3 Laser cooling of trapped ions

3.1 Doppler cooling

- If the recoil frequency $\omega_{rec} = \hbar k_L^2/2m \ll \Gamma$, then the usual Doppler cooling process works and the semi-classical treatment can be applied.
- If $\omega_{x,y,z} \ll \Gamma$ one absorption/emission cycle occurs in a time a lot shorter than the oscillation periods, the ion velocity does not change much during one cycle and the continuous force model explaining Doppler cooling limit can be applied.

$$\begin{array}{ccccccc} \Gamma_{gm} & < & \omega_{rec} & < & \omega_{x,y,z} & < & \Gamma_{ge} \\ \simeq 1 \text{ Hz} & & \simeq 10 \text{ kHz} & & \simeq 1 \text{ MHz} & & \simeq 10 \text{ MHz} \end{array}$$

- For the experiments we are interested in, it is very important that $\omega_{rec} \ll \omega_{x,y,z}$ as $\eta = k_L x_0 = \sqrt{\omega_{rec}/\omega_{x,y,z}}$.
- DA transition $|g\rangle \rightarrow |e\rangle$ are used for Doppler cooling whereas the DF transition $|g\rangle \rightarrow |m\rangle$ are used for QI, metrology...
- Contrary to neutral atom Doppler cooling, a single direction of propagation is enough to cool trapped ions, as long as this direction has projection on all the symmetry axis of the trap. Nevertheless, there are several reasons that can prevent laser cooled ions to reach the Doppler limit...

3.1.1 Excess micromotion

If bias voltage builds up in the trap, the pseudopotential center is shifted from the node of the electric field. Then, the ion oscillates around a shifted position:

$$x(t) = (X \cos \omega_x t + \epsilon_x)(1 + \frac{q_x}{2} \cos \Omega t) \tag{54}$$

this gives rise to an excess contribution to the velocity which is driven by the rf field. It can be nulled only by applying compensation voltages to side electrodes. But a diagnostic is required to evaluate ϵ_x, let's mention

1. *the rf correlation technique*: by a time to amplitude converter (TAC), you look for a modulation at frequency Ω in the DA transition fluorescence. It is the method to start with as it does not requires very cold ions. The limitation is that to have information on excess micromotion in 3D, three directions of propagation are needed. Some setups only offer partial information.
2. *the resolved sideband spectra* where the Ω band is the signature of excess micromotion. To be relevant, this method must be applied to an ion already close to the Lamb-Dicke regime.

3.1.2 Having several sidebands inside the Doppler spectrum

Even if the motional sidebands are not resolved ($\Gamma \gg \omega$), the quantum treatment of the motion inside the laser coupling Hamiltonian can be applied. In our usual approximations (travelling wave, low micromotion regime, Lamb-Dicke regime), but without neglecting the micromotion, the first order expansion in η of $\hat{V}^I$ is (work of Cirac, Garay, Blatt, Parkins and Zoller in 1994)

$$\hat{V}^I = \frac{\hbar\Omega_L}{2}|e\rangle\langle g|\left(\hat{1}e^{-i(\delta t-\psi)} + i\eta\sum_{-\infty}^{\infty} C_{2n}\left(\hat{a}^\dagger e^{-i(\delta-\omega-n\Omega)t-\psi} + i\eta\hat{a}e^{-i(\delta+\omega+n\Omega)t-\psi}\right) + H.c.\right) \tag{55}$$

This equation is an extension of the formulae developped for a perfect H.O, taking into account micromotion and the C_{2n} are the ones already met in the solution of the Mathieu equation. They give the relative amplitude of each motional band $\omega + n\Omega$.

The bands excited when $\delta = -\omega + n\Omega$ leads to cooling whereas the band excited when $\delta = +\omega + n\Omega$ leads to heating (even if $n < 0$). In the very realistic case where $\Gamma/2 \simeq \Omega$, when the laser detuning is chosen for Doppler cooling $\delta \simeq -\Gamma/2$ the heating band at $-\Omega + \omega$ is excited and it works against the cooling process induced on the other bands (the most important one being the $-\omega$ band). This extra heating process do not prevent global cooling but it can prevent the ion to reach the Doppler limit.

When it is not the case, experiments have shown that usual Doppler cooling rules apply. For an example, an experiment performed at the NIST group in 1995 (D. Wineland and coworkers) with a Be^+ ion ($\Gamma/2\pi = 20$ MHz) in a miniature rf-trap ($\Omega/2\pi = 230$ MHz, $\omega/2\pi = 11.2$ MHz) showed that for $\delta \simeq -\Gamma/2$, the measured averaged vibrationnal number is 0.47(5) where the expected number for the Doppler limit is 0.484. Notice that this configuration is ideal for Doppler cooling as $\omega \simeq \Gamma/2$.

What is the expected averaged vibrational number at the Doppler limit?

$$\overline{n} = \frac{e^{-\hbar\omega/k_B T_D}}{1 - e^{-\hbar\omega/k_B T_D}} = \frac{e^{-2\omega/\Gamma_{DA}}}{1 - e^{-2\omega/\Gamma_{DA}}} \tag{56}$$

In the limit where $\omega \ll \Gamma_{DA}/2$, it takes the simple form $\overline{n} = \Gamma_{DA}/2\omega$ which is of the order of 10, at the most.

Historically, the first demonstrations of laser cooling on an ion cloud were reported in 1978 (but not to the Doppler limit) for 50 Ba^+ ions in a rf trap by Toschek, Dehmmelt and coworkers and for Mg^+ ions in a Penning trap by D. Wineland, Drullinger and coworkers at NBS (now NIST) (see bibliography for references).

3.2 Resolved sideband cooling

If the effective linewidth of the transition satisfies $\Gamma_e \ll \omega_{x,y,z}$, then the motional sidebands are resolved and it is possible to tune the laser on the first red sideband (1RSB) to cool the vibrational motion until $\overline{n} \to 0$, if no heating couterbalance this cooling. The spirit of sideband cooling is to excite the ion on a transition where one phonon ($\hbar\omega$) is missing

to the atomic energy transition. Once excited, the ion emits spontaneously a photon. To reach an efficient cooling, the emitted photon must have the atomic transition energy $\hbar\omega_0$ so the system has to be already in the Lamb-Dicke regime. If not, the probability for the photon to be emitted with energy $\hbar(\omega_0 - \omega)$ is non negligeable and several absorption-emission cycles do not result in cooling.

More precisely, the efficiency of SB cooling can be estimated in the non saturated regime, by rate equations, assuming the system is in the LD regime and that the laser is tuned on the 1RSB ($\delta = -\omega$). This work is due to S. Stenholm in 1986 (RMP) and keeps coupling in the lowest order in η. It assumes that $W(\delta) = \Gamma_e^2/(4\delta^2 + \Gamma_e^2)$ is the linewidth profile without saturation, that for absorption on sideband, the relevant η is $(\mathbf{k}_L.\mathbf{x})x_0$ if we are interested in the cooling of the x-motion. But for spontaneous emission on sidebands, the effective η_e has to take into account that only a fraction of the mean squared wavevector project along Ox : $\langle k_x^2\rangle_{es} = \alpha\langle k_L^2\rangle$ and then $\eta_e^2 = \alpha(k_L x_0)^2$.

Let's call $R^{\pm}$ the rate for transition from $|g, n\rangle$ to $|g, n \pm 1\rangle$. In the lowest order in η, R^+ results from the sum of two processes : excitation to $|e, n\rangle$ followed by relaxation to $|g, n+1\rangle$ and excitation to $|e, n+1\rangle$ followed by relaxation to $|g, n+1\rangle$. This writes

$$R^+ = W(\delta)\frac{\Omega_L^2}{\Gamma_e^2} \times \Gamma_e\eta_e^2(n+1) + W(\delta-\omega)\frac{\Omega_L^2\eta^2(n+1)}{\Gamma_e^2} \times \Gamma_e \quad (57)$$

$$= \frac{\Omega_L^2}{\Gamma_e}\left(\eta_e^2 W(\delta) + \eta^2 W(\delta-\omega)\right)(n+1) = A^+(n+1). \quad (58)$$

As for R^-, the same points lead to:

$$R^- = W(\delta)\frac{\Omega_L^2}{\Gamma_e^2} \times \Gamma_e\eta_e^2 n + W(\delta+\omega)\frac{\Omega_L^2\eta^2 n}{\Gamma_e^2} \times \Gamma_e \quad (59)$$

$$= \frac{\Omega_L^2}{\Gamma_e}\left(\eta_e^2 W(\delta) + \eta^2 W(\delta+\omega)\right)n = A^- n. \quad (60)$$

From these two rates, one can calculate the time evolution of the averaged vibrational number in the ground state [1]:

$$\frac{\mathrm{d}\overline{n}}{\mathrm{d}t} = R^+(+1) + R^-(-1) = A^+(\overline{n}+1) - A^-\overline{n} \quad (61)$$

$$= (A^+ - A^-)\overline{n} + A^+. \quad (62)$$

Notice that for $\delta < 0$, $A^- > A^+$. The time evolution is then

$$\overline{n}(t) = \overline{n_0}e^{-(A^- - A^+)t} + \overline{n_f}(1 - e^{-(A^- - A^+)t}) \quad (63)$$

with $\overline{n_f} = 1/(A^-/A^+ - 1)$. If $\delta = -\omega$ and $\omega^2 \gg \Gamma_e^2$

$$A^+ = \frac{\Omega_L^2\Gamma_e}{4\omega^2}\left(\eta_e^2 + \frac{\eta^2}{4}\right) \quad \text{and} \quad A^- = \frac{\Omega_L^2}{\Gamma_e}\eta^2 \quad (64)$$

[1] this is a simplified equation based on the linearity of the rates with n but you can do the full calculation with each n and its probability of occupation $P(n)$, you'll end with the same differential equation for $\overline{n}$

one can see that $A^- \gg A^+$ and the reached mean vibrational number takes the simple form

$$\overline{n_f} \simeq \frac{A^+}{A^-} = \frac{\Gamma_e^2}{4\omega^2}\left(\frac{1}{4} + \frac{\eta_e^2}{\eta^2}\right). \tag{65}$$

The main conclusion is that for resolved sideband cooling, the final vibrational state is described by $\overline{n_f}$ which scales like $(\Gamma_e/2\omega)^2 \ll 1$, to compare to the mean occupation number reached by Doppler cooling $\overline{n_D} \simeq \Gamma_{DA}/2\omega$.

The first experiment in which the motional ground state was reached by RSBC was performed on a single Hg^+ ion, in 1989, at the NIST group (J. Bergquist, W. Itano, D. Wineland and coworkers). The RSBCooling was using a quadrupolar electric transition, broadened by coupling on a dipole transition with an extra laser, to make the cooling faster.

3.3 Cooling a chain of ions

In a linear trap, if $\omega_z < \omega_x, \omega_y$, when cooled down, the ions form a chain at the node of the electric field (the symmetry axis). More precisely if $\omega_{x,y} > \omega^c \simeq 3N/(4\sqrt{\ln N})\omega_z$ the stable configuration is a line. When $\omega_{x,y}$ becomes smaller than ω^c there is a transition to a zig-zag configuration and if $\omega_{x,y}$ is further lowered, the ions move to an helicoidal structure. In practise, for high precision spectroscopy application, the trap is operated to have a line as a stable configuration. To reach such a configuration, the kinetic energy must be lowered so the Coulomb repulsion can be strong enough to lead to a self organisation of the system. For an infinite sample, it was shown a long time ago that, the phase transition to crystals appear for

$$\Gamma_{plasma} = \frac{Q^2}{4\pi\epsilon_0 a}/k_B T \leq 174 \tag{66}$$

with a the mean distance between ions. When the system is finite, this criterium is modified, but still, a phase transition occurs for a given temperature that can be reached by Doppler cooling (the order of 10-100 mK). Then the line is characterized by a nonuniform density which means that distance between ions increase to the border of the trap and then no Bloch theorem or other nice theorem related to periodicity can be used.

Resolved sideband cooling is also very efficient on a chain of ions but now the relevant frequencies of oscillation in the trap are the common vibrational modes. In 1998, the NIST group (D. Wineland and coworkers, Boulder, Colorado) managed to cool the collective modes of motion of two Be^+ (Raman transition) in an elliptical trap which is elongated along the Ox axis. The two ions common mode were then (c.o.m for center of mass)

$$\begin{array}{rcl} \text{c.o.m}_x & \omega_{com} & = \omega_x \\ \text{stretching}_x & \omega_{str} & = \sqrt{3}\omega_{com} \\ \text{c.o.m}_y & & = \omega_y \\ \text{c.o.m}_z & & = \omega_z \\ x-y \text{ rocking} & & = \sqrt{\omega_y^2 - \omega_x^2} \\ x-z \text{ rocking} & & = \sqrt{\omega_z^2 - \omega_x^2} \end{array}$$

When illuminating by a laser beam, the internal states cannot be considered independantly because an excitation on a vibrational sideband on one ion will modify the **common** vibrational state. So the states that must be considered now are of the form

$$|g, g, n_{com}\rangle \quad \text{or} \quad |g, e, n_{str}\rangle.$$

For one ion, on the 1RSB along Ox, $\Omega_{n_x,n_x-1} = \eta_x\sqrt{n_x}\Omega_L$. For two ions, excitation on the 1RSB along Ox, the effective Rabi frequency for the coupling is $\sqrt{2(2n_x-1)}\eta_x^{'}\Omega_L$ where $\eta_x^{'}$ depends on the excited vibrational mode:

- for c.o.m, $\eta_x^{'} = \eta_x/\sqrt{2}$ as $x_0^{'} = x_0/\sqrt{2}$ for $m \to 2m$.
- for stretching mode, $\eta_x^{'} = \eta_x/\sqrt{2\sqrt{3}}$ as $x_0^{'} = x_0/\sqrt{2\sqrt{3}}$ for $m \to 2m$ and $\omega_x \to \sqrt{3}\omega_{com}$.

Notice that for $n \to n \pm 1$, only one atom changes its internal state:

$$|g, g, n\rangle \to |g, e, n \pm 1\rangle \quad \text{or} \quad |e, g, n \pm 1\rangle$$

As the frequencies of the different modes are different, the RSBCooling has to act sequentially on each band. For the experiment mentionned above, the results were consistent with a thermal state with

$$\overline{n}_{com} = 0.11^{+0.17}_{-0.03} \Rightarrow n = 0 \text{ for } 90\%^{+3}_{-12} \text{ of time} \quad (67)$$

$$\overline{n}_{str} = 0.01^{+0.08}_{-0.01} \Rightarrow n = 0 \text{ for } 99\%^{+1}_{-7} \text{ of time} \quad (68)$$

the difference between the two modes can be explained by their different symmetry (it takes an asymmetric perturbation to heat an asymmetric mode).

One could think that it is sufficient to cool the vibrational modes of interest and ignore the other ones but if they are not cold enough, these other modes can alter the laser coupling, to second order in η. Let's imagine mode 2 is not cooled so down whereas we want to excite $n \to n^{'}$ on mode 1. Then one can show that the effective Rabi frequency for this coupling is

$$\Omega_{n_1,n_1^{'}}(n_2) = \Omega_L\eta_1\sqrt{n_{1>}}e^{-(\eta_1^2+\eta_2^2)/2}(1 - n_2\eta_2^2) \quad (69)$$

So experiments are not reproductible if n_2 is let to warm up.

Sharing a common vibrational mode allows to entangle internal states of several ions by entangling their internal and external degrees of freedom. This results in one of the most striking application of trapped ions: Creation of entangled states for Quantum Computation gates.

4 Examples of experiments with trapped ions

4.1 Entanglement with trapped ions

4.1.1 Controlled-NOT gate with a single ion

The idea of using a trapped ion system to implement a quantum computer was suggested by I. Cirac and P. Zoller in 1995. It initiated large efforts to realize fundamental quantum logic gates based on entanglement. The first entanglement with trapped ion was realised between the internal and external degree of freedom of a single Be^+ ion in 1995 in the NIST group (C. Monroe, D. Wineland and coworkers). In this experiment, the controlled NOT gate is operated with the control qubit being the vibrational state $|0\rangle$ or $|1\rangle$ and the target qubit being the internal state $|g\rangle$ or $|e\rangle$. So the relevant basis set contains 4 eigenstates :

$$\{|0,g\rangle; |0,e\rangle; |1,g\rangle; |1,e\rangle\}$$

By laser pulses (on Raman pulses in the case of Be^+) tuned on the red sideband, it is possible to coherently couple $|0,e\rangle$ and $|1,g\rangle$ whereas on the blue sideband the coupling is between $|0,g\rangle$ and $|1,e\rangle$. From that, one can realize the basis brick for a quantum computer: the controlled NOT gate. It requires that the ion is first cooled in the vibrational ground state with a high probability. The following sequence is the one used in the experiment mentionned above but other sequences can be used, depending on the internal structure of the atom.

1. the first step is a $\pi/2$ pulse on the carier ($\Omega_L T = \pi/2$ at $\delta = 0$). It creates a linear superposition of $|g\rangle$ and $|e\rangle$.

2. then, there is a 2π pulse on the blue sideband between $|e\rangle$ and an auxiliary state $|aux\rangle$. Its effect is to modify the sign of $|1,e\rangle$ only.

3. finally, a second $\pi/2$ pulse on the carier is applied, dephased by π compared to the first one.

init	$\pi/2$ CB		2π BSB AUX-e		$\pi/2$ CB'	final
$\|g\rangle\|0\rangle$	$\rightarrow$	$\frac{+\|g\rangle+\|e\rangle}{\sqrt{2}}\|0\rangle$	$\rightarrow$	$\frac{+\|g\rangle+\|e\rangle}{\sqrt{2}}\|0\rangle$	$\rightarrow$	$\|g\rangle\|0\rangle$
$\|e\rangle\|0\rangle$	$\rightarrow$	$\frac{-\|g\rangle+\|e\rangle}{\sqrt{2}}\|0\rangle$	$\rightarrow$	$\frac{-\|g\rangle+\|e\rangle}{\sqrt{2}}\|0\rangle$	$\rightarrow$	$\|e\rangle\|0\rangle$
$\|g\rangle\|1\rangle$	$\rightarrow$	$\frac{+\|g\rangle+\|e\rangle}{\sqrt{2}}\|1\rangle$	$\rightarrow$	$\frac{+\|g\rangle-\|e\rangle}{\sqrt{2}}\|1\rangle$	$\rightarrow$	$\|e\rangle\|1\rangle$
$\|e\rangle\|1\rangle$	$\rightarrow$	$\frac{-\|g\rangle+\|e\rangle}{\sqrt{2}}\|1\rangle$	$\rightarrow$	$\frac{-\|g\rangle-\|e\rangle}{\sqrt{2}}\|1\rangle$	$\rightarrow$	$\|g\rangle\|1\rangle$

When conparing the initial and final states, one can see the truth table of the controlled gate: When the vibrational level is $|0\rangle$, the internal state is not modified, on the contrary, when the vibrational level is $|1\rangle$, the internal state is modified. The role of the $\pi/2$ pulse is to build a quantum state sensitive to a modification of the sign on one internal state.

4.1.2 Controlled-NOT gate with two ions

The idea here is that the common vibrational mode is only used to entangle states but is not part of the truth table anymore. Here, the control qubit is ion_1 whereas the target qubit is ion_2. This was first realized in the group led by R.Blatt in Innsbruck in 2003 (F. Schmidt-Kaler and coworkers). To work, the gate has to start with the ions cooled to the vibrational ground state.

1. the first step is a π pulse on ion_1, on the 1BSB. The purpose of this step is to copy the internal state of ion_1 onto the vibrational state, it is called the SWAP operation.

2. the second step is a controlled-NOT gate like explained above, between the common vibrational mode and the internal state of ion_2.

3. the last step is a π pulse on the 1BSB, π dephased compared to the first pulse.

init	π_1 BSB		CNOT ion_2		π_1 BSB'	final
$\|g_1g_2\rangle\|0\rangle$	$\rightarrow$	$\|e_1g_2\rangle\|1\rangle$	$\rightarrow$	$\|e_1e_2\rangle\|1\rangle$	$\rightarrow$	$\|g_1e_2\rangle\|0\rangle$
$\|g_1e_2\rangle\|0\rangle$	$\rightarrow$	$\|e_1e_2\rangle\|1\rangle$	$\rightarrow$	$\|e_1g_2\rangle\|1\rangle$	$\rightarrow$	$\|g_1g_2\rangle\|0\rangle$
$\|e_1g_2\rangle\|0\rangle$	$\rightarrow$	$\|e_1g_2\rangle\|0\rangle$	$\rightarrow$	$\|e_1g_2\rangle\|0\rangle$	$\rightarrow$	$\|e_1g_2\rangle\|0\rangle$
$\|e_1e_2\rangle\|0\rangle$	$\rightarrow$	$\|e_1e_2\rangle\|0\rangle$	$\rightarrow$	$\|e_1e_2\rangle\|0\rangle$	$\rightarrow$	$\|e_1e_2\rangle\|0\rangle$

One notice that the common vibrational state is not part of the truth table of the gate, it is only a mean to entangle ions internal state. Like expected, the internal state of ion_1 controls the modification of ion_2. This example of controlled gate gives you the spirit of controlled entanglement of ions for quantum computation. Many more sophisticated gates have been demonstrated since and now people are able to realise gates with 8 ions.

4.2 High precision metrology with entangled ions

Trapped single ions are among the best candidates for optical frequency standard as they can be trapped and interrogated for a very long time in a very well controlled environment. Techniques of quantum information processing can be used to increase the fidelity of the detection. This is very useful if the clock qubit does not have an efficient cycling transition (or its wavelength is unreachable) and/or if the shelving technique does not result in a 100% detection efficiency.

The first example of such an application is the Al^+/Be^+ clock developped at NIST. Al^+ is a very good candidate on the metrological point of view as it does not suffer (or far less than usual ion) from the systematic shifts that are responsible for the finite accuracy of other ion clocks (quadrupole shift, black body radiation shift...). But on a detection and cooling point of view, it is a bad choice and its internal state is hard to detect with the conventional quantum jump techniques: Be^+ ion is here to play that role, the internal state of Al^+ is read on Be^+ after entanglement of these two ions.

Here is the measurement sequence: it implies Al^+ internal states:

$$|g\rangle = |^1S_0, F = 5/2, m_F = 5/2\rangle \quad (70)$$

$$|e\rangle = |^3P_0, F = 5/2, m_F = 5/2\rangle \quad \tau = 21s \quad (71)$$

For Be^+ internal states, they are two sublevels of the ground state coupled by Raman coupling:

$$|\downarrow\rangle = |^2S_{1/2}, F = 2, m_F = -2\rangle \quad (72)$$

$$|\uparrow\rangle = |^2S_{1/2}, F = 1, m_F = -1\rangle \quad (73)$$

1. Doppler cooling on Be^+ ion, Al^+ cooled by sympathetic cooling.
2. Resolved sideband cooling of the axial modes to vibrational ground state, using the Raman coupling in Be^+.
3. Preparation of Be^+ in state $|\downarrow\rangle$.
4. Al^+ is excited by the clock laser and is left in the coherent superposition $\alpha|g\rangle + \beta|e\rangle$.
5. This internal state is maped onto the vibrational state by a π pulse on the BSB coupling $|0\rangle|g\rangle$ to $|1\rangle|aux\rangle$.
6. The motional state information is transferred to Be^+ internal state using a π pulse on the transition $|1\rangle|\downarrow\rangle \rightarrow |0\rangle|\uparrow\rangle$. So finally the Al^+ and Be^+ are entangled

$$(\alpha|g\rangle + \beta|e\rangle)\,|\downarrow\rangle \rightarrow \alpha|aux\rangle|\uparrow\rangle + \beta|e\rangle|\downarrow\rangle \quad (74)$$

7. The internal state of Be^+ is measured by the quantum jump technique which projects its state into $|\downarrow\rangle$ with probability $|\beta|^2$ or $|\uparrow\rangle$ with probability $|\alpha|^2$. In the first case, the Al^+ state is projected onto $|e\rangle$, in the second case, onto the manyfold $(|aux\rangle, |g\rangle)$.

A single round has a fidelity of measurement 0.85, which is low. But by repeating the measurement and processing some real time analysis, the fidelity reaches 0.9994. This technique allows to reach a relative systematic uncertainty of $2,3.10^{-17}$ on the Al^+ clock frequency measurement (at 267 nm). With the conventional optical Hg^+ clock in NIST this uncertainty is $1,9.10^{-17}$ (at 282 nm) which represents a better precision but this clock is a far older project than the Al^+/Be^+ clock so people expect the precision of this younger project to be improved in the future. The comparison of these two clocks also infer their stability to $2,8.10^{-15}/\sqrt{\tau(s)}$.

Another application of entanglement related to metrology, is the preparation of entangled ions in a decoherence-free subspace to reach higher precision on a measurement. This has been achieved in the Innsbruck group with two calcium ions $^{40}Ca^+$ in Zeeman sublevels of the metastable state: $|D_{5/2}, m_J\rangle$. The purpose is to measure precisely the electric quadrupole of level $|D_{5/2}\rangle$ which is responsible for one of the major systematic

frequency shift on the clock transition by its coupling to electric field gradient. With a single ion, the precision of this measurement is reduced by the fluctuations of the first order Zeeman effect. By building the two ions Zeeman state

$$|\psi\rangle = \frac{1}{\sqrt{2}}\left(|-5/2\rangle_1|+3/2\rangle_2 + |-1/2\rangle_1|+1/2\rangle_2\right), \tag{75}$$

the total Zeeman number for each part of these linear combination is -1 so these two parts are not dephased by a first order Zeeman shift (this subspace is protected from decoherence induced by first order Zeeman effect). On the contrary, as the quadrupole shift depends on $J(J+1)-3m_J^2$, it is negative for the first term of the linear combination and positive for the second. So this effect induces a dephasing between these two parts which can be measured by interferometric method (like Ramsey fringes). This method allowed to gain an order of magnitude in the estimation of the quadrupole, compared to the conventional method where the frequency shift is measured for different applied electric field gradients.

4.3 Sympathetic cooling

The end of the lesson was devoted to application of sympathetic cooling, for few ions and also for large samples. In both cases it allow, for example, to cool molecular ions and study cold chemical reactions. Several examples of reactions are presented. It is important to note that sympathetic cooling is very efficient to cool the translation degree of motion (to typically 10-100 mK) even if the mass ratio and the number ratio between the two species is very high, but it is unefficient for cooling vibration and rotation of molecular ions.

After looking at different examples of experimental realisation, the lesson concludes on the peculiarity of the quadrupole geometry compared to the multipole one and tries to show how different the dynamics and statistics are in both cases.

Here are the notations used during the lessons:

notation	unit	definition
m	kg	mass of the trapped particule
Q	C	charge of the trapped particule
Ω	s^{-1}	radiofrequency of the confining electric field
Φ	V	electric potential created by a voltage applied on a set of electrodes
ω, $\omega_{x,y,z}$	s^{-1}	oscillation frequency in the harmonic pseudo-potential
$a_{x,y,z}$, $q_{x,y,z}$	ND	parameters of the Mathieu equation
λ	m	wavelength of the considered transition
k,k_L	m^{-1}	associated wavevector
x_0	m	size of the wavepacket in the vibrational ground state
η	ND	the Lamb-Dicke parameter $k_L.x_0$
ω_0	s^{-1}	frequency of atomic transition
ω_L	s^{-1}	frequency of the laser
δ, δ_L	s^{-1}	detuning between laser and atomic transition: $\omega_L - \omega_0$
Γ	s^{-1}	natural width of the transition
Ω_L	s^{-1}	Rabi frequency or coupling strength in an atom-laser interaction

Here is a short bibliography to start with. Most groups make their papers available from their website.

1 All you want to know about radiofrequency traps

References

[1] Wolfgang Paul. Electromagnetic traps for charged and neutral particles. *Rev. Mod. Phys.*, 62(3):531–540, 1990. (the Nobel lecture)

[2] P. K. Gosh. *Ion traps*. Oxford university press, 1995.

[3] D. Gerlich. Inhomogeneous rf fields: a versatile tool for the study of processes with slow ions. In Cheuk-Yiu Ng and Michael Baer, editors, *State-selected and state-to-state ion-molecule reaction dynamics, Part I*, volume 82 of *Advances in Chemical Physics Series*. John Wiley and Sons, 1992.

[4] M. Drewsen and A. Brøner. Harmonic linear paul trap: Stability diagram and effective potentials. *Phys. Rev. A*, 62(4):045401, 2000.

2 Laser cooling of trapped ions

[5] W. Neuhauser, M. Hohenstatt, P.E. Toschek, and H.G. Dehmelt. Optical-sideband cooling of visible atom cloud confined in parabolic well. *Phys. Rev. Lett.*, 41:233–236, 1978.

[6] D. J. Wineland, R. E. Drullinger, and F. L. Walls. Radiation-pressure cooling of bound resonant absorbers. *Phys. Rev. Lett.*, 40(25):1639–1642, 1978.

[7] D. J. Wineland and Wayne M. Itano. Laser cooling of atoms. *Phys. Rev. A*, 20(4):1521–1540, 1979.

[8] Wayne M. Itano and D. J. Wineland. Laser cooling of ions stored in harmonic and penning traps. *Phys. Rev. A*, 25(1):35–54, 1982.

review about laser cooling of trapped ions :

[9] J. Eschner, G. Morigi, F. Schmidt-Kaler, and R. Blatt. Laser cooling of trapped ions. *J. Opt. Soc. Am. B*, 20:1003, 2003.

general review about the quantum dynamics of single trapped ions:

[10] D. Leibfried, R. Blatt, C. Monroe, and D. Wineland. Quantum dynamics of single trapped ions. *Rev. Mod. Phys.*, 75(1):281–324, 2003.

2.1 Toward ion crystals

[11] F. Diedrich, E. Peik, J. M. Chen, W. Quint, and H. Walther. Observation of a phase transition of stored laser-cooled ions. *Phys. Rev. Lett.*, 59(26):2931–2934, 1987.

[12] D. J. Wineland, J. C. Bergquist, Wayne M. Itano, J. J. Bollinger, and C. H. Manney. Atomic-ion Coulomb clusters in an ion trap. *Phys. Rev. Lett.*, 59(26):2935–2938, 1987.

[13] M. G. Raizen, J. M. Gilligan, J. C. Bergquist, W. M. Itano, and D. J. Wineland. Ionic crystals in a linear Paul trap. *Phys. Rev. A*, 45(9):6493–6501, 1992.

2.2 Resolved sideband cooling of single ion and chain of ions

[14] D. J. Wineland, Wayne M. Itano, J. C. Bergquist, and Randall G. Hulet. Laser-cooling limits and single-ion spectroscopy. *Phys. Rev. A*, 36(5):2220–2232, 1987.

[15] F. Diedrich, J. C. Bergquist, Wayne M. Itano, and D. J. Wineland. Laser cooling to the zero-point energy of motion. *Phys. Rev. Lett.*, 62(4):403–406, 1989.

[16] B. E. King, C. S. Wood, C. J. Myatt, Q. A. Turchette, D. Leibfried, W. M. Itano, C. Monroe, and D. J. Wineland. Cooling the collective motion of trapped ions to initialize a quantum register. *Phys. Rev. Lett.*, 81(7):1525–1528, 1998.

[17] H. Rohde, S. T. Gulde, C. F. Roos, P. A. Barton, D. Leibfried, J. Eschner, F. Schmidt-Kaler, and R. Blatt. Sympathetic ground state cooling and coherent manipulation with two-ion-crystals. *J. Opt. B*, 3:S34, 2001.

2.3 Cooling with quantum interference (EIT cooling)

[18] G. Morigi, J. Eschner, and C. Keitel. Ground state laser cooling using electromagnetically induced transparency. *Phys. Rev. Lett.*, 85(21):4458, 2000.

[19] C. Roos, D. Liebfried, A. Mundt, F. Schmidt-Kaler, J. Eschner, and R. Blatt. Experimental demonstration of ground state cooling with electromagnetically induced transparency. *Phys. Rev. Lett.*, 85(26):5547, 2000.

[20] G. Morigi. Cooling atomic motion with quantum interferences. *Phys. Rev. A*, 67:033402, 2003.

3 Entanglement and quantum logic with trapped ions

[21] J. I. Cirac and P. Zoller. Quantum computations with cold trapped ions. *Phys. Rev. Lett.*, 74(20):4091–4094, 1995.

[22] C. Monroe, D. M. Meekhof, B. E. King, W. M. Itano, and D. J. Wineland. Demonstration of a fundamental quantum logic gate. *Phys. Rev. Lett.*, 75(25):4714–4717, 1995.

[23] Q. A. Turchette, C. S. Wood, B. E. King, C. J. Myatt, D. Leibfried, W. M. Itano, C. Monroe, and D. J. Wineland. Deterministic entanglement of two trapped ions. *Phys. Rev. Lett.*, 81(17):3631–3634, 1998.

[24] Ch. Roos, Th. Zeiger, H. Rohde, H. C. Nägerl, J. Eschner, D. Leibfried, F. Schmidt-Kaler, and R. Blatt. Quantum state engineering on an optical transition and decoherence in a Paul trap. *Phys. Rev. Lett.*, 83(23):4713–4716, 1999.

[25] D. Leibfried, E. Knill, S. Seidelin, J. Britton, R. B. Blakestad, J. Chiaverini, D. B. Hume, W. M. Itano, J. D. Jost, C. Langer, R. Ozeri, R. Reichle, and D. J. Wineland. Creation of a six-atom 'schrodinger cat' state. *nature*, 453:4091, 2005.

[26] H. Häffner, W. Hansel, C.F. Roos, J. Benhelm, D. Chak al kar, M. Chwalla, T. Körber, U.D. Rapola nd M. Riebe, P.O. Schmidt, C. Becher, O. Gühne, W. Dür, and R. Blatt. Scalable multiparticule entanglement of trapped ions. *nature*, 438: page 643, 2005.

[27] M. D. Barrett, J. Chiaverini, T. Schaetz, J. Britton, W. M. Itano, J. D. Jost, E. Knill, C. Langer, D. Leibfried, R. Ozeri, and D. J. Wineland. Deterministic quantum teleportation of atomic qubits. *nature*, 429:737, 2004.

[28] M. Riebe, H. Haffner, C. F. Roos, W. Hansel, J. Benhelm, G. P. T. Lancaster, T. W. Korber, C. Becher, F. Schmidt-Kaler, D. F. V. James, and R. Blatt. Deterministic quantum teleportation with atoms. *nature*, 429:734, 2004.

3.1 Using entangled states for high precision metrology

[29] D. J. Wineland, J. J. Bollinger, W. M. Itano, F. L. Moore, and D. J. Heinzen. Spin squeezing and reduced quantum noise in spectroscopy. *Phys. Rev. A*, 46(11):R6797–R6800, 1992.

[30] D. B. Hume, T. Rosenband, and D. J. Wineland. High-fidelity adaptive qubit detection through repetitive quantum nondemolition measurements. *Physical Review Letters*, 99(12):120502, 2007.

[31] T. Rosenband, D. B. Hume, P. O. Schmidt, C. W. Chou, A. Brusch, L. Lorini, W. H. Oskay, R. E. Drullinger, T. M. Fortier, J. E. Stalnaker, S. A. Diddams, W. C. Swann, N. R. Newbury, W. M. Itano, D. J. Wineland, and J. C. Bergquist. Frequency ratio of Al+ and Hg+ single-ion optical clocks; metrology at the 17th decimal place. *science*, 319:1808, 2008.

[32] C.F. Roos, M. Chwalla, K. Kim, M. Riebe, and R. Blatt. 'designer atom' for quantum metrology. *nature*, 443: p316,2006.

[33] M. Chwalla, K. Kim, T. Monz, P. Schindler, M. Riebe, C.F. Roos, and R. Blatt. Precision spectroscopy with two correlated atoms. *Appl. Phys. B*, 89:p483,2007.

4 Cooling of large samples and phase transition

[34] R. Blümel, J.M. Chen, E. Peik, W. Quint, W. Schleich, Y.R. Shen, and H. Walther. Phase transition of stored laser-cooled ions. *nature*, 334:309, 1988.

[35] M. Drewsen, C. Brodersen, L. Hornekær, J. S. Hangst, and J. P. Schifffer. Large ion crystals in a linear paul trap. *Phys. Rev. Lett.*, 81(14):2878–2881, 1998.

4.1 Sympathetic cooling

[36] P. Bowe, L. Hornekær, C. Brodersen, M. Drewsen, J. S. Hangst, and J. P. Schiffer. Sympathetic crystallization of trapped ions. *Phys. Rev. Lett.*, 82(10):2071–2074, 1999.

[37] K. Mølhave and M. Drewsen. Formation of translationally cold $MgH+$ and $MgD+$ molecules in an ion trap. *Phys. Rev. A*, 62(1):011401, 2000.

[38] M. D. Barrett, B. DeMarco, T. Schaetz, V. Meyer, D. Leibfried, J. Britton, J. Chiaverini, W. M. Itano, B. Jelenković, J. D. Jost, C. Langer, T. Rosenband, and D. J. Wineland. Sympathetic cooling of $^{9}Be+$ and $^{24}Mg+$ for quantum logic. *Phys. Rev. A*, 68(4):042302, 2003.

[39] B Roth, A Ostendorf, H Wenz, and S Schiller. Production of large molecular ion crystals via sympathetic cooling by laser-cooled Ba+. *J. Phys. B*, 38:3673, 2005.